A novel approach (the CRATER method) for assessing tsunami vulnerability at the regional scale using ASTER imagery

Filippo Dall'Osso[1,3], Lorenza Bovio[3], Alessandra Cavalletti[2,3], Francesco Immordino[3, 4], Marco Gonella[1,3] and Giovanni Gabbianelli[1]

[1] CIRSA, Interdepartmental Centre for Environmental Science Research, University of Bologna – 163, via S. Alberto, 48100 Ravenna, Italy. E-mail: filippodallosso@gmail.com

[2] IDRA, Institute for Environmental Research - 37, via Kennedy, 44100 Ferrara, Italy

[3] MED INGEGNERIA S.r.l. Environmental Engineering - 37, via Kennedy, 44100 Ferrara, Italy

[4]ENEA, Italian National Agency for New Technologies, Energy and Sustainable Economic Development – 4, via Martiri di Montesole, 40129 Bologna, Italy.

Abstract

We present here a novel method to assess coastal vulnerability to tsunami based on GIS (Geographical Information System), ASTER imagery (Advanced Spaceborn Thermal Emission and Reflection Radiometer) and SRTM-3 elevation model (Shuttle Radar Topography Mission-3). We developed this method within the CRATER project (Coastal Risk Analysis for Tsunamis and Environmental Remediation) and applied it on the whole western coast of Thailand. As result, we generated a set of vectorial vulnerability maps with a geometrical resolution of 90m (scale 1:450 000). This approach provides a low-cost and quick tool to analyse extended coastal tracts, and prioritize investments for prevention measures or for further high-resolution analysis.

Keywords: Tsunami, Coastal Vulnerability, ASTER, GIS, Land Use.

Un nuovo approccio (metodo CRATER) per la stima a scala regionale della vulnerabilità a tsunami mediante immagini ASTER

Riassunto

Il lavoro presentato introduce un nuovo metodo per la stima della vulnerabilità costiera a tsunami, basato sul GIS (Geographical Information System), sull'impiego di immagini ASTER (Advanced Spaceborn Thermal Emission and Reflection Radiometer) e modelli di elevazione SRTM-3 (Shuttle Radar Topography Mission–3). Il metodo è stato sviluppato nell'ambito del progetto CRATER (Coastal Risk Analysis for Tsunamis and Environmental Remediation) ed applicato all'intera costa occidentale della Tailandia. I risultati consistono in un set di mappe vettoriali della vulnerabilità con risoluzione di 90m (scala 1:450 000). Tale approccio costituisce un mezzo relativamente economico e veloce per l'analisi di estesi tratti costieri e per la gestione di investimenti in misure di prevenzione o in ulteriori analisi ad alta risoluzione.

Parole chiave: *Tsunami, Vulnerabilità costiera, ASTER, GIS, Uso Suolo.*

Introduction

There are many definitions of vulnerability, but at the broadest level, it is agreed as meaning "potential for damage". Godshalk [1991] describes vulnerability as "the susceptibility to injury or damage from hazards", while according to Mitchell and Cutter [1997] vulnerability is "the potential for loss or the capacity to suffer harm from a hazard. It can generally be applied to individuals, society, or the environment". The United Nations [1992] describe vulnerability as the "degree of loss (from 0% to 100%) resulting from a potentially damaging phenomenon".

The Indian Ocean Tsunami (IOT) of December 2004 clearly demonstrated that a large teletsunami can have major impacts on low lying coastal areas of those countries that surround the entire ocean basin. Furthermore, depending on local socio-economic and environmental conditions, the vulnerability to, and impacts of a tsunami at any given location can be highly variable even along a few kilometres of coastline [UNEP, 2005].

The 2004 IOT caused highly variable damage within the coastal zones of nine countries from South East Asia (Indonesia, Thailand, Myanmar, Bangladesh, Sri Lanka, India, Maldives) to Eastern Africa (Kenya and Somalia) more than 4500 km from its source [Titov et al., 2005; Lovholt et al., 2006; Matsutomi and Sakakyama., 2006; Nadim and Glade, 2006; Thanawood et al., 2006].

Given the potential scale of the affects of tsunamis and the high spatial variability of the caused damage, local and national government agencies faced with the task of developing appropriate tsunami disaster risk reduction strategies need appropriate tools to enable them to assess vulnerability at various scales. National and local administrations need specific tools to analyse existing vulnerability, prioritize prevention measures and address available financial resources in most critical areas.

For a tsunami of any given magnitude, the vulnerability of exposed coastal areas may be estimated by taking into consideration all human and environmental factors that contribute to the expected level of damage. The choice of factors that can/should be analysed is dependent on the scale and the accuracy of the results required by decision makers. For example, the vulnerability of a single building may be assessed via an analysis of factors related to its physical features (e.g., construction material, number of stories). Conversely, assessment of the vulnerability of an entire coastal region requires other datasets at completely different scales (e.g., land cover, coastal geomorphology). Consequently, the types and scales of analysis influence the volumes and accuracy of data needed. Outputs from the vulnerability assessment process can be easily displayed via simple, clear thematic maps [Cutter et al., 2003; Williams and Alvarez, 2003].

At present, available methods for tsunami vulnerability assessment are designed to be applied mainly at high resolution [Papadopoulos and Dermentzopoulos, 1998; Papathoma et al., 2003; Papathoma and Dominey-Howes, 2003; Aitkenhead et al., 2007; Dominey-Howes and Papathoma, 2007; Garcin et al., 2008; Taubenbock et al., 2008; Dall'Osso et al., 2009a; Dall'Osso et al., 2009b; Dominey-Howes, et al., 2010] using data at the scale of individual buildings or infrastructure units. Data are normally gathered through field surveys and direct census analysis. Due to their high resolution and the time required for data collection, these methods are well suited to the analysis of vulnerability 'hot spots' such as limited portions of urbanised areas or single villages. Those hot spots must be chosen among all exposed coastal sites, on the basis of specific Public Administrations (PA)

requests, or scientific interests based on past tsunamis.
At the other end of the spatial scale, analysis at regional or national levels use satellite imagery or geographic data to identify and map areas that are exposed to tsunami flooding [Theilen-Willige, 2006; Chandrasekar et al., 2007;Theilen-Willige, 2008]. However, within those areas, the vulnerability level depends also on the environmental and socio-economic variability, which is not considered by most of such approaches. Land cover data were considered by Wood [2009], in a study aimed at identifying the tsunami prone land along the Oregon coast of the United States. Wood extracted land cover data from ETM+ sensor (Landsat satellite) images and coupled these with pre-existing tsunami-hazard information. Although this approach is one of the few to consider the integration of socio-economic and environmental data, it is based on the use of a pre-existing database of tsunami hazard information which is highly unlikely to be available elsewhere, making the application of Wood's approach problematic.
This paper outlines an innovative new method for undertaking rapid, regional to national scale assessments of coastal vulnerability to tsunamis that may be applied anywhere. The data needed to undertake the vulnerability analysis are easily gathered from readily available ASTER satellite images (Advanced Spaceborn Thermal Emission and Reflection Radiometer) and 3s-SRTM-v3 (3 arc-seconds Shuttle Radar Topography Mission, version 3) digital elevation models. Results of the vulnerability assessment can be displayed via GIS as a series of thematic maps having an horizontal resolution of 90 m (scale of 1:450 000). Our approach goes beyond that of Wood [2009] as it exploits the flexibility and higher resolution of the newer ASTER sensor. It has wide applicability since it is not based on the need for detailed tsunami hazard or tsunami inundation zones.
We applied our new method to the entire western coast of Thailand as part of the CRATER Phase II (Coastal Risk Analysis for Tsunamis and Environmental Remediation) project. In the 2004 IOT aftermath, the CRATER project represented the technical contribution of the Italian Government to Thailand. Because of the large geographic region involved in the original CRATER project, the coast of Thailand was divided in to 12 separate mapped areas. However, here we just present a case study of Phuket Island to illustrate the capability of our approach. Readers interested in the results for the other coastal zones of Thailand zones can contact the authors and ask for the CRATER final report.
For our inundation scenario we considered a single wave (rather than wave train) generating a run-up up to 25 m a.m.s.l. (above mean sea level) inundating to a distance of 5 km. Given the characteristics of the inundation generated by the 2004 IOT [Titov et al, 2005; Lovholt et al., 2006; Siripong, 2006; Hori et al., 2007] we consider this to be the "worst credible case" for a tsunami affecting the west coast of Thailand.

The CRATER Method

Measuring the vulnerability level: required data

Data contributing to the general vulnerability level has been chosen and evaluated on the basis of the analysis scale, the extent of the study area, and previous post-tsunami surveys. We analysed the vulnerability of coastal zones and inland areas using the following parameters:
- for coastal zones: infrastructural, geomorphological and ecological features;
- for inland areas: land use, altimetry and distance from the shoreline.

Coastal zones

According to field surveys undertaken after the 26th of December IOT, the highest damage occurred in urbanised areas (harbors, wharfs, aquaculture plants), especially if located behind long and flat shorelines [Darlymple and Kriebel, 2005; Ghobarah et al., 2006; Matsutomi and Sakakyama, 2006; Thanawood et al., 2006]. In particular, beaches experienced very high changes during backwash, which eroded sediment and deposited it over coral reefs [UNEP, 2005]. This scouring effect appeared to be more evident for long and wide-open beaches in flat areas, rather than in small bays with pocket beaches. Strand and Masek [2005] suggested that this could be due to the higher amount of water flowing inland and back to the sea after the inundation. Coastal geomorphology was found to be an important factor controlling the tsunami effects also by Nainarpandian et al. [2007].

Another key-role of coastal ecological features was played by mangrove forests, that suffered some damages from the wave impact and the strong sedimentation rate, but also behaved as a protection for inland areas. Mangrove roots and branches reduced the flow velocity and trapped sediment and debris [UNEP, 2005; EJF, 2006; Chang et al., 2006; Bhalla , 2007; Cochard et al., 2008; Rabindra et al., 2008].

Inland areas

The vulnerability of inland areas is strictly dependent on the overall value of each land portion that could be partially or completely damaged during the inundation. That value includes socio-economic aspects (population, buildings, economic resources) and environmental features (natural resources) [Wood, 2009]. Given our scale of analysis, we considered land use as a proxy for the overall value of inland areas.

The inland topography (intended as elevation above mean sea level) was also considered as a basic element for understanding what will be the depth of water during inundation at any particular point within the study area.

Finally, the distance from the shoreline was also considered as a factor affecting the vulnerability of inland areas because of the dissipation of the water flow energy, caused the friction effect of soil during the inundation [Iverson and Prasad, 2007].

Data gathering and analysis: ASTER imagery and SRTM elevation model

We used a set of 15 daytime ASTER images to extract information about coastal geomorphology, land use and distance from the shoreline along the entire western coast of Thailand. Phuket Island was fully covered by a single image, taken on the 8th of February 2005 (Fig. 1).

The ASTER sensor consists of three different subsystems : the Visible and Near-infrared (VNIR) has three bands with a spatial resolution of 15 m, and an additional backward telescope for stereo; the Shortwave Infrared (SWIR) has 6 bands with a spatial resolution of 30 m; the Thermal Infrared (TIR) has 5 bands with a spatial resolution of 90 m [Abrams and Hook 1998; Abrams, 2000; Yamaguchi et al., 2001]. Each image covers an area of 60 km x 60 km and the repeat cycle is 16 days.

Data about topography was obtained through the use of a 3s SRTM-v3 Digital Elevation Model (DEM), version-3. SRTM is an interpherometric DEM produced by NASA (http://seamless.usgs.gov/products/srtm3arc.php#download). The SRTM DEM we used has a horizontal geometrical resolution of 90 m and a reported vertical accuracy of 10 m (root

mean square error). Version 3 has been adjusted for radar speckle errors that often affect coastal flat areas. SRTM DEM have been effectively used in several flood studies [Theilen-Willige, 2006; Demirkesen et al., 2007]. Sanders [2007] compared performances of SRTM DEM with other types of on-line available DEMs and highlighted utility of SRTM data as a global source for flood modelling purposes, especially after correction for radar speckle errors. Furthermore, the SRTM vertical accuracy for relatively flat terrain was found to be better than in high relief areas, which is advantageous for coastal flood studies [Sanders, 2007].

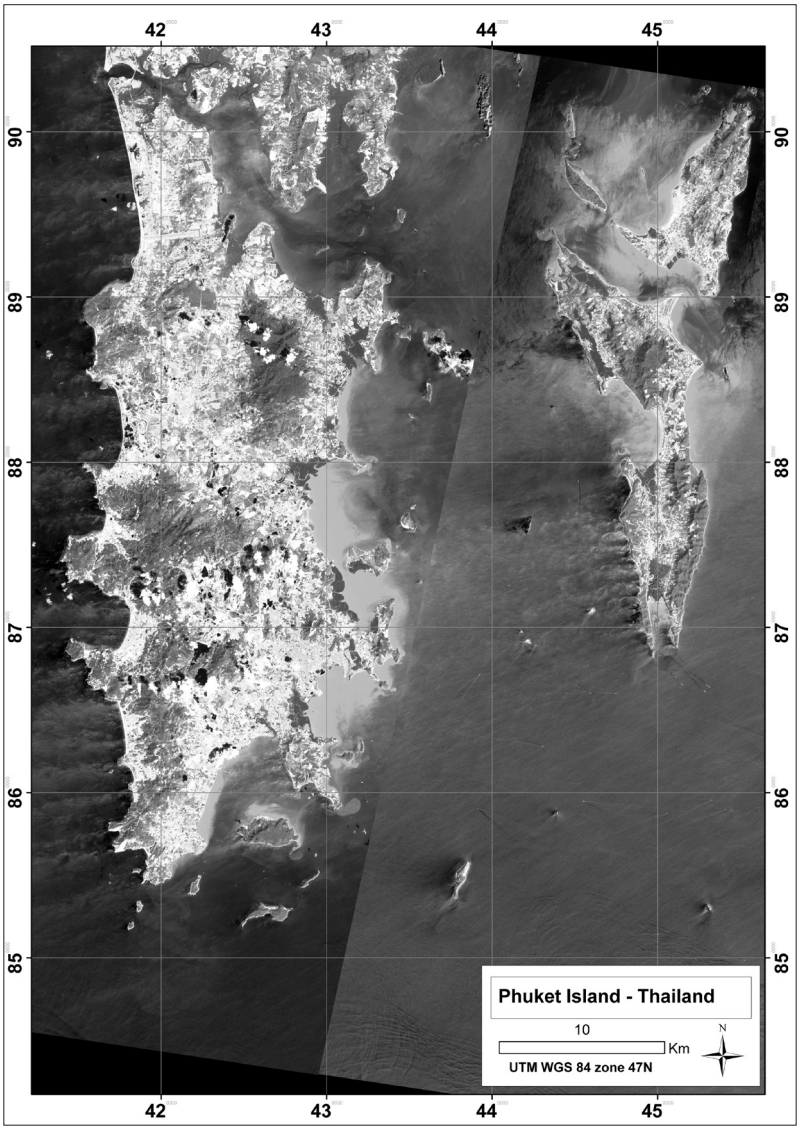

Figure 1 – The ASTER image used for Phuket Island (colour composite scheme RGB: 3N, 2, 1).

Coastal zones

We extracted data about coastal zones via a visual photo-interpretation of the ASTER images. We digitized the whole coastline and divided it into six geomorphologic classes expressing different vulnerability levels to tsunami. Photo-interpretation was undertaken at the maximum detail level allowed by ASTER band 1 to 3N (15 m), which is consistent with our scale of analysis. We assigned each class a vulnerability score (CV, Coastal Vulnerability score) ranging between 1 (minimum vulnerability) and 5 (maximum vulnerability) (Tab. 1). Such scores were assigned on the basis of the damage observed during field surveys carried out after past tsunamis, particularly the 2004 IOT.

Table 1 - Coastal Vulnerability scores (CV) given to each coastline class.

Coastline features:	Infrastructure	Beach and Low Ground	Pocket Beach	Mangroves	High Ground (sea cliff)
CV score:	5	4	3	2	1

Land use

ASTER images have been widely used for the classification of land use type [Jianwen and Bagan, 2005; Buhe et al., 2007; Yuksel et al., 2008], in natural hazard risk analysis [Liu et al., 2004; Hubbard et al., 2007; Kamp et al., 2008], but not to study tsunami vulnerability assessment.

Pre-processing of the ASTER images

This work has been undertaken using ASTER level 1B scenes, that is ASTER level 1A (raw product) corrected from instrumental and geometric errors [ERSDAC, 2000]. All VNIR and SWIR bands of the ASTER image have been resampled to a spatial resolution of 15 m using nearest neighbour resampling process. All the images are projected into Universal Transverse Mercator, Zone 47 N with a WGS-84 datum.

In order to eliminate the effects of atmospheric scattering and absorption in the VNIR and to increase the accuracy of surface type classification [Kaufman,1985; Falkowski et al. 2005], the DN values have been converted to TOA (Top Of the Atmosphere) reflectance. This procedure is divided in two steps: (1) Converting DN values to spectral radiance; (2) Transferring the sensor detected radiance into TOA reflectance.

At the first step, DN values of the sensor measurements are converted into spectral radiance measured (L_{rad}) by satellite sensor using the following equation:

$$L_{rad} = (DN - 1) \cdot c \quad [1]$$

where c is the unit conversion coefficient which differs for each ASTER band.

Within this study, the normal values of c (Tab. 2) for each band were obtained from the ASTER user's guide [Abrams and Hook, 1998].

In step number (2), we applied an Atmospheric correction to the ASTER satellite images using the "Fast Line-of-sight Atmospheric Analysis of Spectral Hypercubes (FLAASH)" of the ENVI software. FLAASH incorporates the MODTRAN 4 radiation transfer code

with all MODTRAN atmosphere and aerosol types to calculate a unique solution for each image.
The input radiance image is converted in BIL (Band Interleaved by Line) or BIP (Band Interleaved by Pixel) format to get the radiance value in floating-point.
A tropical atmosphere parameter (columnar water vapour content 4.11 g cm^{-2}) and marine aerosols together with automatic aerosol retrieval are used in FLAASH to correct the ASTER image.

Table 2 - The unit conversion coefficients for the operating bands of ASTER

Band	Coefficient [W/(m² · sr · μm)]/DN			ESUNi (W·m⁻²·μm⁻¹)
	High gain	Normal	Low gain	
1	0.676	1.688	2.25	1847
2	0.708	1.415	1.89	1549
3N	0.423	0.862	1.15	1114
3B	0.423	0.862	1.15	1114
4	0.1087	0.2174	0.2900	225.4
5	0.0348	0.0696	0.0925	86.63
6	0.0313	0.0625	0.0830	81.85
7	0.0299	0.0597	0.0795	74.85
8	0.0299	0.0417	0.0556	66.49
9	0.0159	0.0318	0.0424	59.85

Classification

The classification process we adopted is based on a pixel-oriented approach, where each pixel is assigned to a class of land cover based on image spectral information.
In the present work, the classification was undertaken using the "decision tree" tool of the ENVI software. Such tool consists of a number of connected classifiers (i.e. decision nodes) which perform jointly the pixel classification task through a multistage process made-up of a series of binary decisions (Fig. 2). Each decision is here based on a numerical comparison with a selected threshold index, which makes the whole process easily repeatable. Despini et al. [2009a, b] have recently used a similar method to extract land use classes from MODIS images. The main advantage of such approach is that data from many different sources and files can be used together to make a single decision tree classifier. Furthermore, the "decision tree" tool is non parametric, therefore it makes no assumptions on the distribution of the input data [Friedl and Brodley, 1997].
The indexes chosen for the classification process are reported in Table 3: the NDVI is a simple numerical indicator that can be used to analyse remote sensing measurements, typically but not necessarily from a space platform, and assess whether the target being observed contains live green vegetation or not; the Albedo (A) is retrieved from the equation below [Liang, 2000]:

$$A = 0.484\rho_1 + 0.335\rho_3 - 0.324\rho_5 + 0.551\rho_6 + 0.305\rho_8 - 0.367\rho_9 - 0.0015 \quad [2]$$

where ρ_1, ρ_3, ρ_5, ρ_6 , ρ_8 and ρ_9 are the reflectance for the corresponding ASTER bands. The

spectral bands used in the "decision tree" are the band 3 (NIR 0.76-0.86μm) and band 4 (MIR = 1.6-1.7μm).

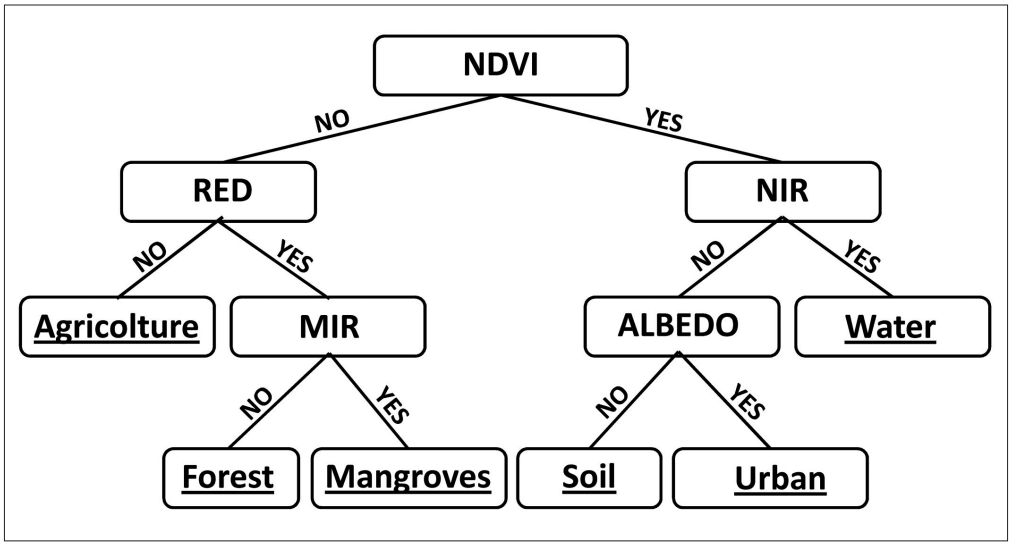

Figure 2 – Overview of the ENVI "Decision Tree" tool used for the classification process. Such tool provides a hierarchical supervised classification made up of a series of binary decisions that are used to determine the correct category for each pixel.

Table 3 – Indexes used for the classification process.

Index	Description
NDVI	NDVI < 0.25
RED	RED < 0.12
NIR	NIR < 0.1
MIR	MIR < 0.012
Albedo	Albedo < 0.3
NDVI 2	0 < NDVI2 < 0.12

We extracted 6 different land use classes: water, urban areas, agriculture, mangroves, forest and soil (Fig. 2). Where present, clouds and cloud shades (where no data was recognizable) have been vectorialised and added to the GIS database.

We verified the reliability of outputs using the confusion matrix method [Van Genderen et al., 1978]. The test areas used for the accuracy evaluation were selected following field surveys undertaken on Phuket Island in 2005.

After the classification process, we divided those areas classified as being "urbanised" in two further classes, according to the observed density of buildings. Such classes are: (1) Urbanised Areas (high density) and (2) Urbanised Areas (low density). The division was carried out through a photo-interpretation process. The final land use map is shown in Figure 3.

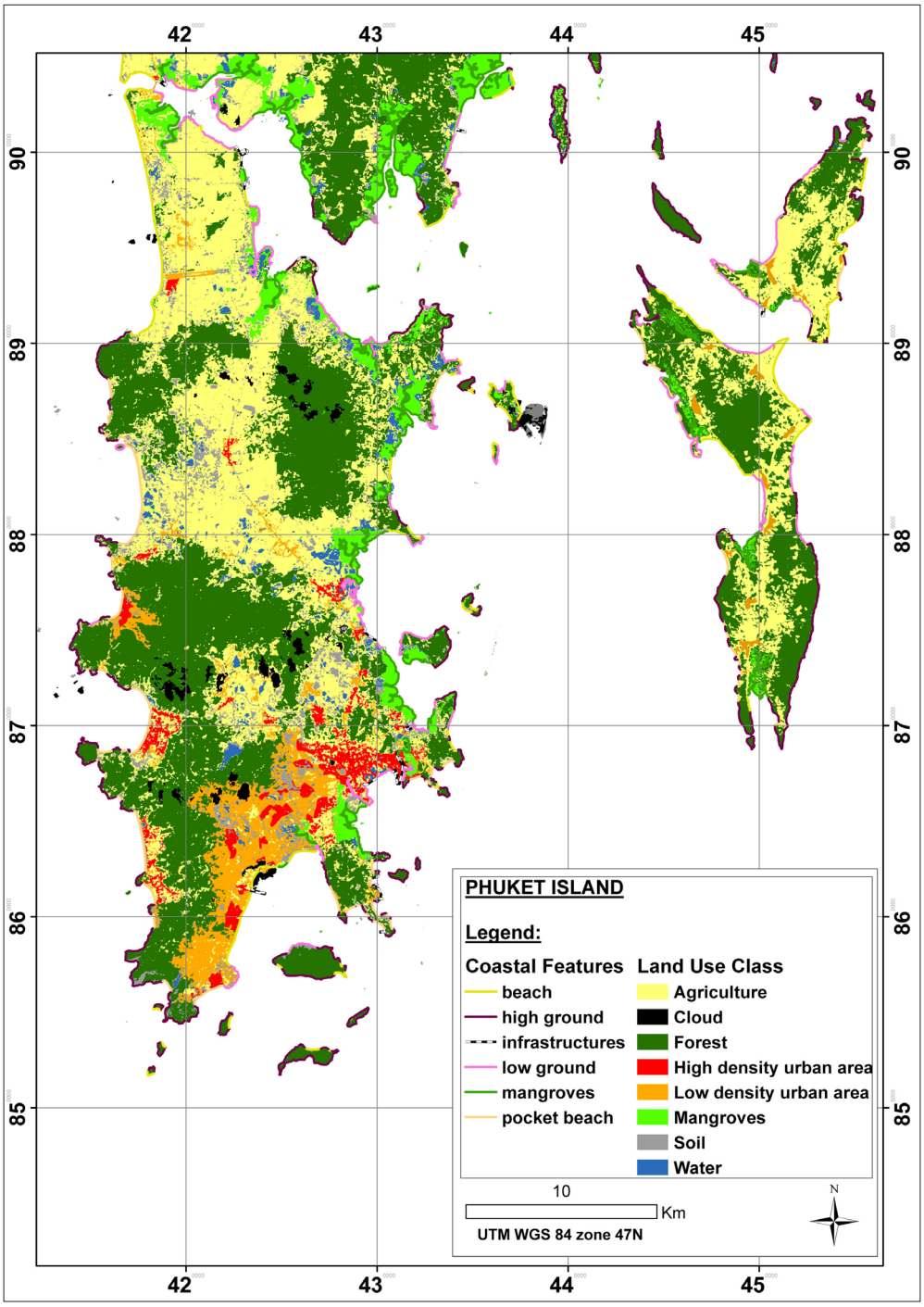

Figure 3 - Land use map of Phuket Island. Results of the photo-interpretation of coastal features are shown with different colours along the shoreline.

Finally, we assigned to each land use class a Land Use Vulnerability score (*LUV*), ranging from 1 to 5 (Tab. 4). Again, LUV scores were assigned according to the damage to different land use types observed after the 2004 IOT. Note that low scores are given to forest and mangroves, because although they have an important natural value, the damages they would suffer have been scaled with respect to those of urbanised areas, that have been considered the most vulnerable. The class "water" includes pools for aquaculture, that together with agriculture is one of the primary economic industries for Thailand. The naked soil class includes beaches and temporarily uncultivated crops. Both aquaculture plants, agricultural crops and beaches suffered heavy damage during the 2004 tsunami [Wartnitchai, 2005, Mapa et al., 2005]. Highest vulnerability scores are assigned to urban areas. To emphasize the difference between the vulnerability of buildings and other land use classes, we left a gap in the scores scale (none of the classes has a vulnerability score of 3).

Table 4 - Land Use Vulnerability scores (*LUV*) given to each land use class.

Land Use classes:	Urbanised Areas (high density)	Urbanised Areas (low density)	Agriculture, Beaches, Aquaculture pools, Lakes and Freshwater	Forest and Mangroves
LUV score:	5	4	2	1

Altimetry

SRTM data were downloaded in a .tiff format and converted to a vectorial dataset through ArcGIS 9.2. The whole study area was divided into cells with sides of 90 metres associated with an average altimetry value expressed in metres above mean sea level (m a.m.s.l.). Since the vertical domain of analysis includes only areas lower than 25 m a.m.s.l., all of the cells up to 25 m a.m.s.l. were extracted from the DEM and displayed in a new map, after being divided into 3 intervals. Elevation Vulnerability scores (EV) were assigned to each interval according to Table 5 (Fig. 4).

Table 5 - EV scores have been given according to the SRTM elevation values.

SRTM Elevation (m a.m.s.l.)	[0-10]	[10-20]	more than 20
EV score	5	3	1

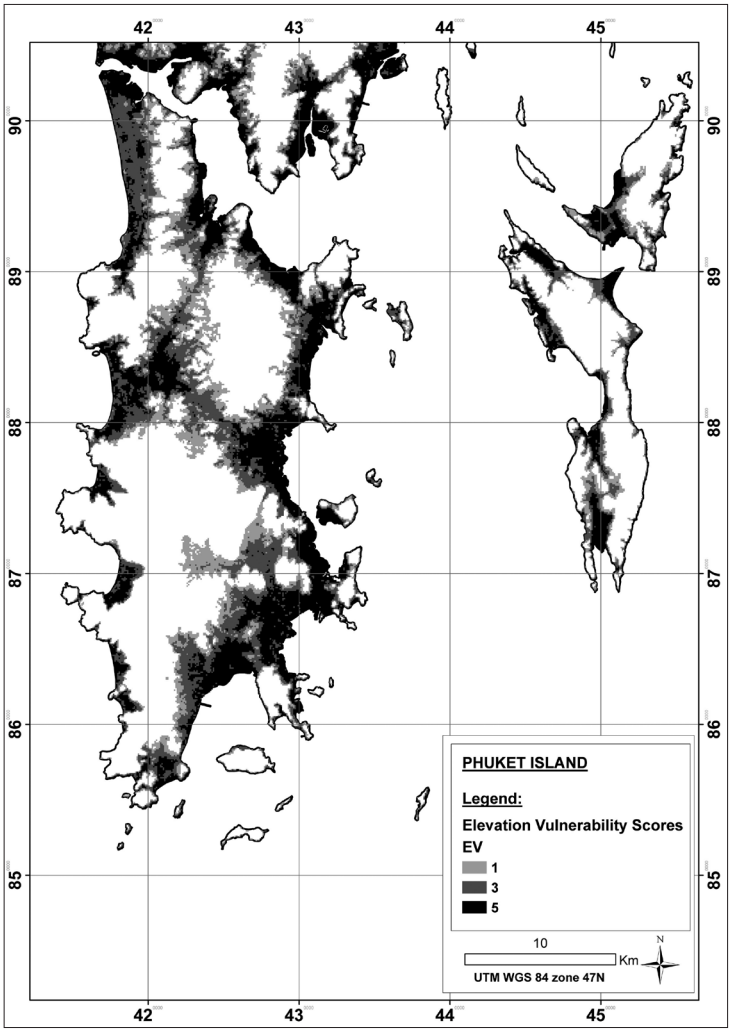

Figure 4 - An "Elevation Vulnerability" score (EV) ranging between 1 and 5 has been given to all zones lower than 25 m a.m.s.l. We set EV intervals according to Table 5.

Distance from the shoreline

Since the maximum wave inundation 2004 exceeded 3 km at Khao Lak, Phang-Nga province [Siripong, 2006], we set the horizontal domain of the analysis to the 5th kilometre inland. Using the ArcGIS 9.2 "buffer" tool, we divided the first 5 kilometres of land into 5 belts, parallel to the shoreline and having each a width of 1 km (Fig. 5). To each belt we gave a Distance Vulnerability score (DV) ranging from 5 (maximum vulnerability, from the shoreline until the 1st kilometre inland) to 1 (minimum vulnerability, from the 4th to the 5th kilometre inland) (Tab. 6).

Table 6 - Vulnerability scores (*DV*) given to different belts of distance from the shoreline.

Distance from the shoreline (km)	[0-1]	[1-2]	[2-3]	[3-4]	[4-5]
DV score:	5	4	3	2	1

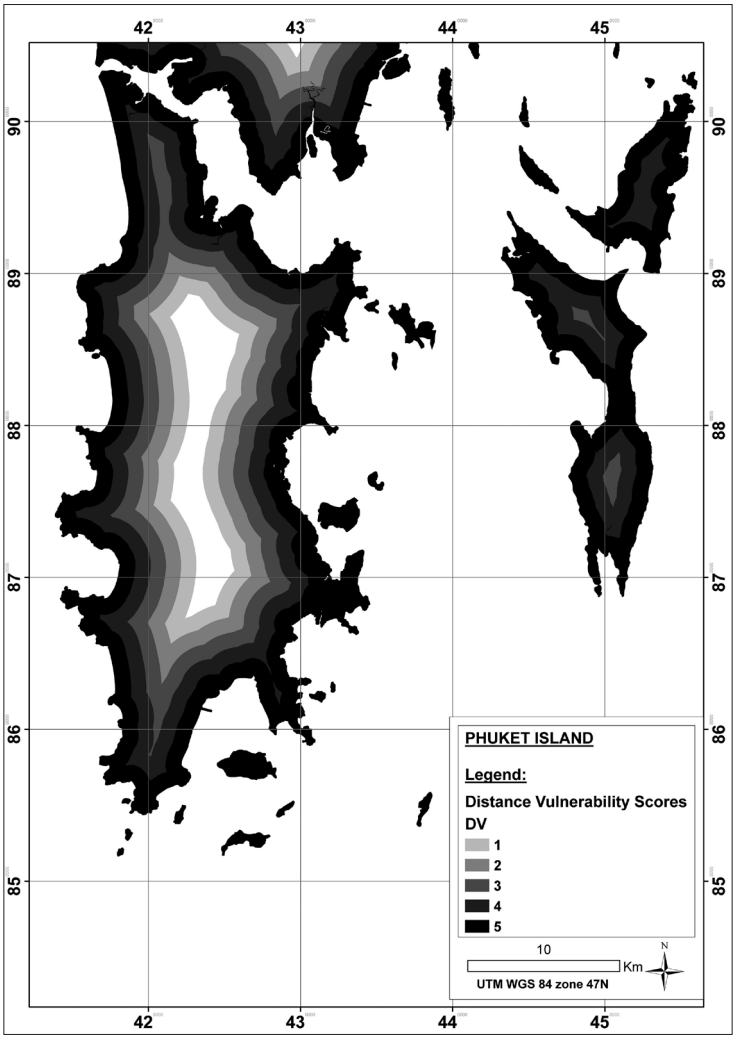

Figure 5 - We divided the first 5 kilometres from the shoreline into 5 belts, each 1-km wide. To every belt we gave a Distance Vulnerability score (DV) ranging from 5 (from the shoreline until the 1st kilometre inland) to 1 (from the 4th to the 5th kilometre inland).

Calculating the overall vulnerability level

We calculated the vulnerability of the coastline and inland areas with two different indexes. The coastline vulnerability index scores are summarized in Table 1.

An overall vulnerability index of inland areas (V_{tot}) was calculated by joining together contributions made by single vulnerability factors (land use, altimetry, distance from the shoreline). This index was assigned to each land portion generated through a geometrical intersection among the three factor maps (Figs. 3, 4, 5). The intersection was executed though the ArcGIS 9.2 tool called "intersect". This process generated a new polygon shapefile, containing only those areas that were common to all the three factor maps. As a consequence, we calculated a V_{tot} value for all of the areas falling within the first 5 kilometres of the shoreline and having a topographical elevation smaller than 25 metres. V_{tot} scores were calculated as follows:

$$V_{tot} = 2\,LUV + EV + DV \qquad V_{tot} \in [4,\ 20] \quad [3]$$

At the moment, no already tested/validated indexes for the assessment of the tsunami vulnerability at a regional scale are available in literature. We gave LUV a weight of 2 because it gives information on both the resilience and the socio-economic value of the exposed areas, while EV and DV just set the domain of the inundation.

Results

Vulnerability scores assigned to different coastal morphologies (CV) and calculated for different type of inland areas (V_{tot}) have been stored into a GIS, together with all inputs and the ASTER image. We used ArcGIS 9.2 to display results in form of vulnerability maps, through a colour-coded scale. Vulnerability scores of inland areas have been divided into 5 equal intervals. That division has been made through one of the different GIS applications for graphic representation on quantitative data. ArcGIS users could display vulnerability scores in a different way without modifying the numerical information on V_{tot}, which is the main result of the analysis. Figure 6 shows the geographic range of those vulnerability classes across all Phuket subdistricts (tambon). The surface extent of different vulnerability classes in every subdistrict is summarized in Table 7.

The most vulnerable areas are located in the southern part of Phuket Island, within the subdistricts of Chalong, Wichit, Talat Nua, Talat Yai and Ratsada, where the city of Phuket is located. In that area most of the inundated zones have "High" and "Very High" vulnerability scores. Excluding the peninsula of Wichit and the mangroves in Ratsada, the coastline vulnerability index (CV) of that area ranges between 4 and 5.

On the east coast, the bays of Karon, Patong, Kamala and Choeng Tale have mainly "High" and "Very High" vulnerability scores. However, the extent of the inundated area is much smaller than at Phuket Town and CV values are average (CV=3).

The inundated areas of Sa Khu and Mai Khao have basically an "Average" V_{tot}, except of the Phuket International Airport, which is located at the boundary between the two subdistricts and has "High" and "Very High" scores. CV values range between 4 and 5, aside from a small mangroves area at north and the promontory in the southern part of Sa Khu, which would not be inundated.

On the north-eastern coast V_{tot} is mainly "Low" to "Average" although it rises to "Very High" at Pa Khlok Town. CV reaches very high (CV=5) scores at several beaches within the subdistrict

of Pa Khlok, as well as at Pa Khlok Town. Within the subdistrict of Ko Kaeo V_{tot} and CV are "High" to "Very High".

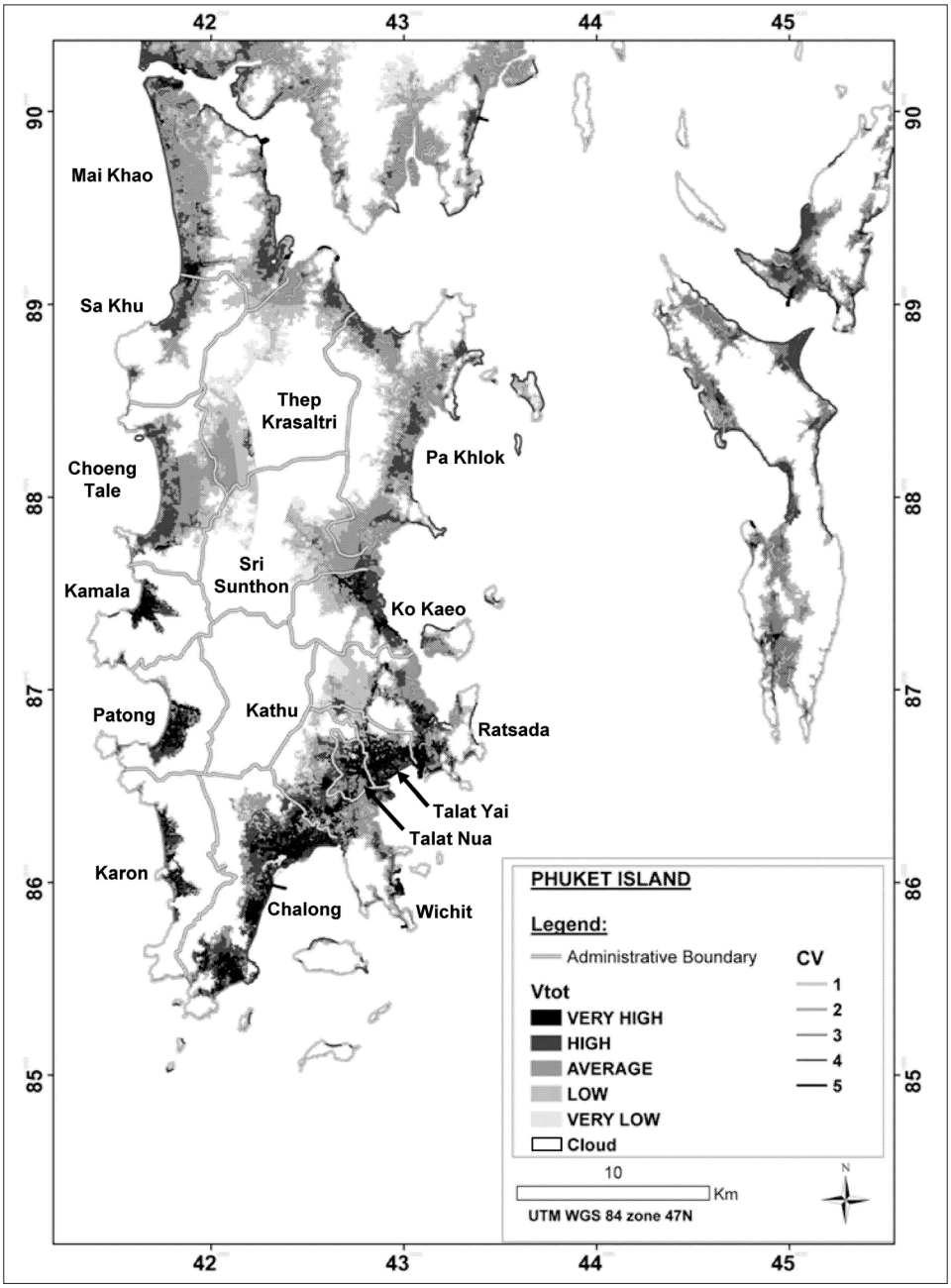

Figure 6 - Vulnerability map generated for Phuket Island, obtained as an intersection of data shown in Figures n 3, 4 and 5. V_{tot} scores are obtained from Equation [3].

Discussion and Conclusion

We developed and described an innovative approach (the CRATER method) that allows to generate tsunami vulnerability maps with a resolution of 90 m covering regional areas. Maps show the patterns of two different tsunami vulnerability indexes: one for coastal zones (CV) and one for inland areas (V_{tot}). End-users will need to consider both indexes to have a general view of the vulnerability distribution across their study area.

Table 7 - Surface extent of different vulnerability classes in each Phuket subdistrict.

Subdistrict	Land surface (Ha) with V_{tot} = [4-7.2] **(VERY LOW)**	Land surface (Ha) with V_{tot} = [7.2-10.4] **(LOW)**	Land surface (Ha) with V_{tot} = [10.4-13.6] **(AVERAGE)**	Land surface (Ha) with V_{tot} = [13.6-16.8] **(HIGH)**	Land surface (Ha) with V_{tot} = [16.8-20] **(VERY HIGH)**
Chalong	58.9	336.5	650.5	956.7	723.28
Choeng Tale	69,7	438.3	852.7	452.4	14.7
Kamala	6.5	65.5	49.7	144.1	127.7
Karon	0.7	102.4	118.4	173.5	117.3
Kathu	0	0	0	0	0
Ko Kaeo	43.0	367.0	371.1	313.3	123.7
Mai Khao	14.2	949.5	1688.6	607.1	82.4
Pa Khlok	252.1	1040.3	1692.3	555.2	0
Patong	0.6	75.0	115.6	174.0	167.8
Ratsada	145.1	747.8	601.2	347.8	179.1
Sa Khu	41.0	308.4	289.2	199.6	12.6
Sri Sunthon	443.6	541.2	369.5	74.3	1.6
Talat Nua	8.7	36.1	149.3	123.3	166.0
Talat Yai	19.5	104.5	124.7	149.7	295.1
Thep Krasaltri	518.0	1048.5	763.5	151.4	0
Wichit	112.2	462.5	716.2	468.0	239.4

We showed an application on Phuket Island, Thailand.
All the inputs (coastal features, land use, altimetry and distance from the shoreline) have been obtained from satellite products (ASTER imagery and SRTM-3 DEM). In particular,

we extracted the required land use classes through a pixel-based classification of the ASTER images, based on the use of the "decision tree" tool (ENVI software) and a set of selected threshold indexes. Such approach ensures the repeatability of the whole classification process in different areas, or in the same areas at a different time.

As shown by the map in Figure 6, most vulnerable inland areas resulted to be located in highly urbanised zones close to the shoreline. However, not all of the urbanised areas have been classified as having the same vulnerability score, since also the altimetry and the distance from the shoreline have been considered in the assessment. Most critical areas are those nearby the city of Phuket (subdistricts of Talat Yai, Talat Nua and Chalong) and all the bays on the western coast (subdistricts of Karon, Patong, Kamala). All these areas are located right on the coast, they have a rather flat topography and an high density of buildings. The only areas in which V_{tot} and CV scores could not be calculated are those covered by clouds at the moment the images were taken. However all the chosen images have a cloud coverage lower than the 10%.

The V_{tot} index we adopted is based on the assumption that the contribution to the overall vulnerability made by different land use types has a weight two times larger than EV and DV (Equation 3). Such approach, plus the criteria used to assign LUV scores in Table 4, allows to emphasize the vulnerability of the exposed urbanised areas against low-lying undeveloped coastal zones, which during the 2004 Indian Ocean Tsunami experienced a much lower damage. To our knowledge, no other indexes for assessing the vulnerability to tsunami at the regional scale are available in literature.

The scenario we adopted consists in a "flat" inundation, given by a single wave hitting every point of the shoreline with the same height and able to reach inland areas located up to 25 m a.m.s.l., within the first 5 km from the shoreline. The choice of assuming the inundation to be "flat" and given by a single wave is an approximation that we assumed to be acceptable, since at the moment this study was undertaken neither a probabilistic tsunami assessment nor a wave numerical simulation were available for such a large area. As a consequence, vulnerability maps that can be created through this approach leave aside the location of the tsunami generation site and the main direction of the tsunami propagation.

However, as demonstrated by the 2004 IOT, Public Administrations and local risk managers need tools to assess the vulnerability to tsunamis now, and cannot wait until probabilistic scenarios and inundation models will be available for their respective areas of interest. The CRATER method may thus find many applications as a precautionary tool for supporting decision makers in long term urban planning and emergency strategies.

The use of remote sensing data allows to asses vulnerability to tsunami on very extended areas, at national or even at ocean basin scale, with a relatively small amount of time and money. To our knowledge, this is the first work aimed to the creation of a methodology for tsunami vulnerability analysis at a regional scale, coupling land use data from ASTER imagery and SRTM-3 topography. Most of the existing methods work at the scale of single building/infrastructure and can be applied only to pre-selected spot areas. A regional scale approach such as the CRATER method may be useful to analyse more extended coastal zones and decide whether and where further high-detail analysis should be undertaken.

Furthermore, because of world-coverage and availability of the input data required, this method can be applied anywhere and it doesn't need any pre-existing information

about tsunami inundation-prone zones.
Finally, the use of GIS allows to generate interactive maps, that can be queried by different type of end – users and easily kept updated through years, which is basic for low-frequency hazards such as tsunamis.

Acknowledgements
We wish to thank Dave Anning and prof. Dale Dominey-Howes for revising an earlier version of this paper. We thank prof. Sergio Teggi and two anonymous referees for their essential technical and scientific contributions.

References

Abrams M., Hook S. (1998) - *ASTER User Handbook, Version 1*. NASA/Jet Propulsion Laboratory, Pasadena.

Abrams M. (2000) - *The Advanced Spaceborne Thermal Emission and Reflection Radiometer (ASTER): data products for the high spatial resolution imager on NASA's Terra platform*. International Journal of Remote Sensing, 21, No. 5: 847 – 859.

Aitkenhead M.J., Lumsdon P., Miller D.R. (2007) - *Remote Sensing-Based Neural Network Mapping Of Tsunami Damage In Aceh, Indonesia*. Disasters, Blackwell Publishing, 31, No.3: 217-226.

Bhalla R. S. (2007) - *Do Bio-Shields Affect Tsunami Inundation?*. Current Science, 93, No. 6.

Buhe A., Tsuchiya K., Kanenko M., Ohtaischi N., Halik M. (2007) - *Land Cover Of Oases And Forest In Xinjiang, China Retrieved From Aster Data*. Advances In Space Research 39: 39-45.

Chandrasekar N., Immanuel J. L., Sahayam J. D., Rajamanickam M., Saravanan S. (2007) - *Appraisal of tsunami inundation and run-up along the coast of Kanyakumari District, India – GIS analysis*. Oceanologia, 49 (3), pp. 397-412.

Chang S. E., Adams B. J., Alder J, Berke P., Chuenpagdee R., Ghosh S., Wabnitz C. (2006)- *Coastal Ecosystems and Tsunami Protection after the December 2004 Indian Ocean Tsunami*. 22, No. S3: S863-S887.

Cochard R., Ranamukhaarachchib S. L., Shivakotib G. P., Shipinb O.V., Edwardsa P. J., Seelandc K. T. (2008) - *The 2004 Tsunami In Aceh And Southern Thailand: A Review On Coastal Ecosystems, Wave Hazards And Vulnerability*. Perspectives in Plant Ecology, Evolution and Systematics, 10: 3-40.

Cutter S.L., Bryan J.B., Shirley W.L. (2003) - *Social Vulnerability to Environmental Hazards*. Social Science Quarterly, 84, No. 2.

Dall'Osso F., Gonella M., Gabbianelli G., Withycombe G., Dominey-Howes D. (2009a) - *A revised (PTVA) model for assessing the vulnerability of buildings to tsunami damage*. Nat. Hazards Earth Syst. Sci., 9: 1557-1565.

Dall'Osso F., Gonella M., Gabbianelli G., Withycombe G., Dominey-Howes D. (2009b) - *Assessing the vulnerability of buildings to tsunami (in Sydney)*. Nat. Hazards Earth Syst. Sci., 9: 2015-226.

Dalrymple R.A., Kriebe D.L. (2005) - *Lessons in Engineering from the Tsunami in Thailand*. The Bridge, 35: 4-13.

Demirkesen A. C., Evrendilek F., Berberoglu S., Kilic S. (2007) - *Coastal Flood Risk Analysis Using Landsat-7 ETM+ Imagery and SRTM DEM: A Case Study of Izmir, Turkey*. Environmental Monitoring And Assessment, 131: 293-300.

Despini F., Teggi S., Bovio L., Immordino F. (2009a) - *Applications of Terra MODIS data for Iraq marshland monitoring.* Proceedings of the SPIE Europe's International Symposium on Remote Sensing (ERS09), 31 August-3 September Berlin.

Despini F., Teggi S., Bovio L., Immordino F. (2009b) - *Applicazioni di immagini MODIS per il monitoraggio delle Marshland Irachene.* 13°Conferenza Nazionale ASITA, 1-4 dicembre 2009, Fiera del Levante – Bari.

Dominey-Howes D., Papathoma M. (2007) : *Validating a Tsunami Vulnerability Assessment Model (the PTVA Model) Using Field Data from the 2004 Indian Ocean Tsunami*. Natural Hazards, 40, 113-136.

Dominey-Howes D., Dunbar P., Verner J., Papathoma-Köhle M. (2010) - *Estimating probable maximum loss from a Cascadia tsunami*. Nat Hazards, 53: 43–61.

ERSDAC (Earth Remote Sensing Data Analysis Center), (2001). *ASTER User_s Guide, Part II, Ver. 3.1.*

EJF (Environmental Justice Foundation) (2006) - *Mangroves: Nature's Defence Against Tsunamis* - A Report On The Impact Of Mangrove Loss And Shrimp Farm Development On Coastal Defences. London.

Falkowski M.J., Gessler P.E., Morgan P., Hudak A., Smith T. (2005) - *Characterizing and mapping forest fire fuels using ASTER imagery and gradient modeling.* Forest Ecology and Management, 217: 129–146.

Friedl M.A., Brodley, C.E. (1997) – *Decision tree classification of land cover from remotely sensed data.* Remote Sensing of Environmental. 61: 399-409.

Garcin M., Desprats J.F., Fontaine M., Pedreros R., Attanayake N., Fernando S., Siriwardana C. H. E. R., De Silva U., Piosson B. (2008) - *Integrated Approach For Coastal Hazards And Risks In Sri Lanka*. Natural Hazards And Earth System Sciences, 8: 577-586.

Ghobarah A., Saatcioglu M., Nistor I. (2006) - *The Impact Of The 26 December 2004 Earthquake And Tsunami On Structures And Infrastructure*. Engineering Structures, 28: 312 – 326.

Godschalk D.R. (1991) - *Disaster Mitigation And Hazard Management. Emergency Management: Principles And Practice For Local Government*. Drabek, E. T. and Hoetmer, G. J. (Eds.), International City Management Association, Washington DC.

Hori K., Kuzumoto R., Hirouchi D., Umitsu M., Janjirawuttikul N., Patanakanog B. (2007) - *Horizontal and vertical variation of 2004 Indian tsunami deposits: An example of two transects along the western coast of Thailand*. Marine Geology; 239: 3-4, 162-172.

Hubbard B. E., Sheridan M. F., Carrasco-Nùnez G., Diaz-Castellòn R., Rodrìguez S.R. (2007) - *Comparative Lahar Hazard Mapping At Volcan Citlaltépetl, Mexico Using Srtm, Aster And Dted-1 Digital Topographic Data*. Journal Of Vulcanology And Geothermal Research, 160: 99-241.

Iverson L.R., Prasad A.M. (2007) - *Using Landscape Analysis To Assess And Model Tsunami Damage In Aceh Province, Sumatra*. Landscape Ecology, 22: 323-331.

Jianwen M., Bagan H. (2005) - *Land-Use Classification Using Aster Data And Self-Organized Neutral Networks*. International Journal Of Applied Earth Observation and Geoinformation, 7: 183-188.

Kamp U., Growley B. J., Khattak G. A., Owen L. A. (2008) - *Gis-Based Landslide Susceptibility Mapping For The 2005 Kashmir Earthquake Region*. Geomorphology, 101: 631-642.

Kaufman Y.J. (1985) - *The atmospheric effect on the separability of field classes measured from satellites.* Remote Sensing of Environment 18: 21-34.

Liang S., Strahler A. (2000) - *Land surface bi-directional reflectance distribution function (BRDF): Recent advances and future prospects*. Special issue of Remote Sensing Reviews, 18: 83-511.

Liu J. G., Mason P. J., Clerici N., Chen S., Davis A., Miao F., Deng H., Liang L. (2004) - *Landslide Hazard Assessment In The Three Gorges Area Of The Yangtze River Using Aster Imagery: Zigui–Badong*. Geomorphology, 61: 171-187.

Lovholt F., Bungum H., HarbitzC.B., Glimsdal S., Lindholm C.D., Pedersen G. (2006) - *Earthquake Related Tsunami Hazard Along The Wastern Coast Of Thailand*. Natural Hazards and Earth System Sciences, 6: 979-997.

Mapa R.B., Wickramasinghe W.M.A.D.B., Sirisena D.N., Kendaragama K.M.A. (2005) - *Salt In The Soil*. Soil Science Society of Sri Lanka.

Matsutomi H. and Sakakyama T. (2006) - *Aspects Of Inundated Flow Due To The 2004 Indian Ocean Tsunami*. Coastal Engineering Journal, 48, No. 2, 167-195.

Mitchell, J.T., Cutter, S.L. (1997) - *Global Change and Environmental Hazards: Is the World Becoming More Disastrous?* Association of American Geographers, Washingston DC.

Nadim F., Glase T. (2006) - *On Tsunami Risk Assessment For The West Coast Of Thailand*. ECI Conference On Geohazards, LilleHammer, Norway.

Nainarpandian C., Jeyakodi L.I., Jeyaraj D. S., Manoharan R., Sakthivel S. (2007) - *Appraisal Of Tsunami Inundation And Run-Up Along The Coast Of Kanyakumari District, India – Gis Analysis*. Oceanologia, 49, No. 3, 397-412.

Papadopoulos A., Dermetzopoulos T. (1998) - *A Tsunami Risk Management Pilot Study in Heraklion, Crete*. Natural Hazards, 18, 91-118.

Richards J. A. (1999) - *Remote Sensing Digital Image Analysis*. Springer-Verlag, Berlin, pp 240.

Papathoma, M., Dominey-Howes, D., Zong, Y., Smith, D. (2003) - *Assessing Tsunami Vulnerability, An Example From Herakleio, Crete*, Natural Hazards and Earth System Sciences, 3: 377-389.

Papathoma, M., Dominey-Howes, D. (2003) - *Tsunami Vulnerability Assessment And Its Implications For Coastal Hazard Analysis And Disaster Management Planning, Gulf Of Corinth, Greece*. Natural Hazards and Earth System Sciences, 3: 733–747.

Rabindra O., Tanak S., Toshikazu T. (2008) - *The Importance Of Mangrove Forest In Tsunami Disaster Mitigation*, The Author(s). Journal compilation, Blackwell Publishing.

Sanders B. F. (2007) - *Evaluation Of On-Line DEMs For Flood Inundation Modelling*. Advances In Water Resources, 30: 1831-1843.

Siripong A. (2006) - *Andaman Seacoast of Thailand Field Survey after the December 2004 Indian Ocean Tsunami*. Earthquake Spectra, 22, No. 3: S187-S202.

Strand C., Masek J., (2005) - *Sumatra – Andaman Islands Earthquake and Tsunami of December 26, 2004 Lifeline Performance*. Technical Council Of Lifeline Eartquake Engineering, Monograph n. 29, October 2005, Cap. 8.

Taubenbock H., Post J., Kiefl R., Roth A., Ismail F.A., Strunz g., Dech S. (2008) - *Risk And Vulnerability Assessment To Tsunami Hazard Using Very High Resolution Satellite Data – The Case Study Of Padang, Indonesia*. Remote Sensing – New Challenges of High Resolution, Bochum.

Thanawood C., Yongchalermchai C., Densrisereekul O. (2006) - *Effects Of The December*

2004 Tsunami And Disaster Management In Southern Thailand. Science of Tsunami Hazards, 24, No. 3: 206-217.

Theilen-Willige B. (2006) - *Emergency Planning In Northern Algeria Based On Remote Sensing Data In Respect To Tsunami Hazard Preparedness*. Science of Tsunami Hazards, 25, No. 1: 3-12.

Theilen-Willige, B. (2008) - *Tsunami Hazard Assessment In The Northern Aegean Sea*. Science of Tsunami Hazards, 27, No. 1: 1-16, 2008.

Titov V., Rabinovich, B. A., Mofjeld, H. O., Thomson, E. R., Gonzalez, F. I. (2005) – *The Global Reach Of The 26 December 2004 Sumatra Tsunami*, Science, 309, 2045, DOI: 10.1126/science.1114576.

UNEP (United Nations Environment Programme) (2005) - *After The Tsunami: Rapid Environmental Assessment*.

United Nations, Department of Humanitarian Affairs (1992) - *Internationally Agreed Glossary of Basic Terms Related to Disaster Management*. Geneva, Switzerland.

Van Genderen J. L., Lock B. F., Vass. P. A. (1978) - *Remote sensing: statistical testing of thematic map accuracy.* Proceedings of the 12th International Symposium on Remote Sensing of Environment, ERIM, Ann Arbor, MI, pp. 3-14.

Warnitchai P. (2005) - *Lessons Learned from the 26 December 2004 Tsunami Disaster in Thailand.* Proceedings of the 4th International Symposium on New Technologies for Urban Safety of Mega Cities in Asia, Singapore, 18-19 October.

Williams A.T., Alvarez R.A. (2003) - *Vulnerability Assessment As A Tool For Hazard Mitigation, Submarine Landslides and Tsunamis*. Kluwe Academic Publisher, Netherlands, 303-313.

Wood N. (2009) - *Tsunami Exposure Estimation With Land Cover Data: Oregon And The Cascadia Subduction Zone*. Applied Geography.

Yamaguchi Y., Fujisada H., Tsu H., Sato I., Watanabe H., Kato M., Kudoh M., Kahle A.B., Pniel M. (2001) - *Aster Early Image Evaluation*. Advanced Space Research, 28, No.1: 69-76.

Yüksel A., Akay A. E., Gundogan R. (2008) - *Using ASTER Imagery in Land Use/cover Classification of Eastern Mediterranean Landscapes According to CORINE Land Cover Project*. Sensors, 8: 1237-1251.

Received 19/01/2010, accepted 25/05/2010.